Smart Health 26 (2022) 100337

Contents lists available at ScienceDirect

Smart Health

journal homepage: www.elsevier.com/locate/smhl

Evaluating melting gel coatings for wearable metabolic sensors

Anthony Annerino [a,*], Kenneth Narvaez [b], Lorne Joseph [b], Lisa C. Klein [b], Pelagia-Irene Gouma [a,c]

[a] Department of Materials Science and Engineering, The Ohio State University, 140 W 19th Avenue, Columbus, OH, 43210, USA
[b] Department of Materials Science and Engineering, Rutgers University, 607 Taylor Road, Piscataway, NJ, 08854, USA
[c] Department of Mechanical and Aerospace Engineering, The Ohio State University, 201 W 19th Avenue, Columbus, OH, 43210, USA

ARTICLE INFO

Keywords:
Wearable sensor
Polyaniline
Melting gel
Composite

ABSTRACT

New steps have been taken toward finalizing a novel wearable sensor for entirely non-invasive, continuous blood sugar monitoring via the low concentrations of acetone continuously emitted from human skin as a byproduct of metabolic activity. This sensor is based on a chemo-mechanical actuating polymer composite of the well-known conducting polymer polyaniline and cellulose acetate, which is a simple derivative of the incredibly proliferous and benign organic compound cellulose. The improvements reported here revolve around the application of a 65% methyltriethoxysilane – 35% dimethyldiethoxysilane melting gel to one side of the sensor, thereby isolating the sensor from ambient air and any interferents it might contain. Visual inspection shows that the melting gel does not prohibit functionality of the existing polyaniline-cellulose acetate sensor, and FTIR spectroscopy shows that no significant chemical changes are caused by application of the melting gel to the polyaniline-cellulose acetate sensor.

1. Introduction

Biomarker sensing has historically focused on breath or sweat (Biscay et al., 2021; Ganguly et al., 2020; Gouma & Stanacevic, 2011; Kang et al., 2016; Klous et al., 2020; Manolis, 1983; Miekisch et al., 2004; Morgan et al., 2004; Mörk & Johanson, 2006; Patterson et al., 2002; Solga et al., 2006; Thirumalaikumar et al., 2021; Toyooka et al., 2013; Turner et al., 2008; Vasilescu et al., 2021; Ye et al., 2015). While these have scientific merit on account of their physical discoveries, new advances in sensing the gases that are continuously and ambiently emitted from the skin hold the most promise for continuous and totally non-invasive health monitoring that can genuinely pull point-of-care health monitoring into the future (Alessi et al., 2017; Bag & Lee, 2021; He et al., 2019; Mojtabavi et al., 2016; Raghu et al., 2019; Singh et al., 2017). Breath monitoring can only be non-invasive or continuous since continuous breath monitoring requires actively sampling every breath and even the smallest devices for breath sensing are large enough to be cumbersome in most situations like that developed by the MIT Lincoln Lab (Candell et al., 2020). Similarly, sweat sensing requires stable quantities of sweat which are difficult to maintain in most real-life situations, and even authors working to get around this such as Ganguly et al. concede that technology coming down the pipeline seems unable to adapt to the influences of other constituents in sweat on a biomarker of interest (Ganguly et al., 2020). The template formats your text by using 'Styles' which define the format (or appearance) of a paragraph of text as regards letter size, indentation, line spacing, etc.

Polyaniline (PANI) is among the very few intrinsically conducting polymers because of its conjugated electron density along its

* Corresponding author.
E-mail address: Annerino.2@osu.edu (A. Annerino).

https://doi.org/10.1016/j.smhl.2022.100337
Received 22 August 2022; Accepted 29 September 2022
Available online 3 October 2022

chain length as depicted in Fig. 1. Cellulose acetate (CA) is derived from cellulose, which is among the least expensive and most benign biopolymers. When processed together, the unique properties of PANI can still be utilized despite PANI's miserable mechanical properties on account of CA's robust mechanical properties (Mojtabavi et al., 2016).

This work specifically aims at taking advantage of the well-established relationship between concentrations of acetone emitted by the human body and blood sugar levels (Turner et al., 2008). Previous work with this material system established sensitivity to acetone, so next steps have been focused on moving forward with assembling a device based on this PANI-CA composite (Annerino et al., 2022).

Such next steps revolved around the investigation of melting gels as a hermetic seal over the top of the PANI-CA composite to protect it from interference from species not emanating from the skin since melting gels have been investigated as hermetic seals on electronic devices and show great promise for applications like this in general (Aparicio et al., 2017; Gambino et al., 2012; Jitianu et al., 2010, 2012; Klein & Jitianu, 2010, 2014). Melting gels are organically modified silicate gels that reversibly stiffen below some material-unique glass transition temperature, typically around 100 °C, but also irreversibly consolidate from cross-linking, typically around 160 °C. The melting gels investigated here involved various ratios of the mono-saturated siloxane methyltriethoxysilane (MTES) and the di-substituted siloxane dimethyldiethoxysilane (DEMDES); these are depicted in Fig. 2.

2. Experimental procedures

2.1. Materials

All melting gels discussed here were prepared using only as-received materials. MTES, ammonia, and anhydrous ethanol were procured from Sigma-Aldrich, Milwaukee, WI. DMDES was procured from Fluka Chemicals, Milwaukee, WI. Hydrochloric acid was procured from Fisher Scientific, Atlanta, GA. Dry acetone was procured from Riedel-de Haën, Seelze, Germany.

2.2. Methods

2.2.1. Melting gel synthesis

Melting gels were synthesized from the precursors by first making separate solutions of MTES in ethanol with distilled water and hydrochloric acid and DMDES in ethanol. Upon combination of these solutions, ammonia was added, and dry acetone was added so the byproduct ammonium chloride could be removed by vacuum filtration. The product was finally dried below its consolidation temperature to remove any residual solvents.

2.2.2. Melting gel characterization

Each melting gel composition has a unique consolidation temperature, which was determined by repeatedly heat cycling it to incrementally higher temperatures above its glass transition temperature then cooling it to room temperature until finding a heat treatment temperature that caused this reversible behavior to stop. Melting gel was applied to previously prepared PANI-CA composite films by warming the melting gel so it flowed then painting it onto the PANI-CA films with a paintbrush. FTIR spectra of both sides of the PANI-CA films were collected before and after the application of the melting gel to one side to evaluate any chemical interaction between the PANI-CA film and the melting gel; this was performed using a ThermoNicolet Avatar 360 FTIR (Waltham, MA) equipped with a Smart Endurance ATR attachment (diamond crystal). Density and specific surface area of the painted-on melting gel film was calculated from nitrogen physisorption measurements taken with a Micromeritics Gemini 2375 Analyzer (Norcross, GA) using the Brunauer–Emmett–Teller method. It was verified that the PANI-CA films still function as acetone sensors after the melting gel was applied by recording videos of them being suspended in the headspace above 50 mL of acetone in a 125-mL conical flask. These recordings were captured with a SONY HandyCam HDR-CX455.

3. Results

The melting gel composition that produced the best adhesion to the PANI-CA samples contained 65% MTES – 35% DMDES. Visual examination was the basis for selecting this composition for further study. The thickness of the melting gel coating depended on the number of times the layer was applied. Typically, only one coating was applied and the layer was about 0.06 mm thick. One sample was prepared with 4 layers, making a total thickness of about 0.12 mm. The coatings are shiny and transparent. A typical sample with one

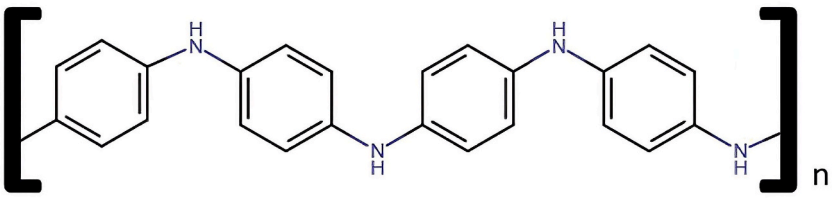

Fig. 1. The leucoemeraldine oxidation state of PANI.

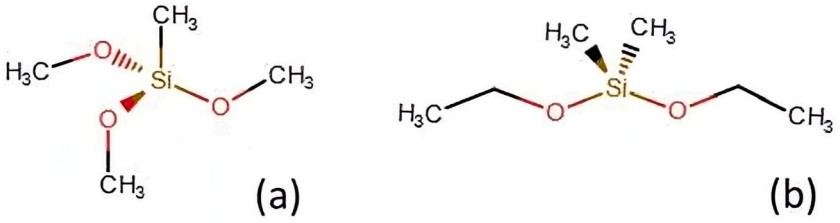

Fig. 2. The structures of methyltriethoxysilane (a) and dimethyldiethoxysilane (b).

layer is shown in Fig. 3. The 65% MTES – 35% DMDES coating is known to have a high value of the contact angle ($\theta = 100°$), a low BET surface area (0.0138 m^2/g) and a low density (1.252 g/cm^3).

FTIR spectra of both sides of the PANI-CA films were collected before and after the application of the melting gel to one side. The spectra were collected to evaluate any chemical interaction between the PANI-CA film and the melting gel. The spectra of the PANI-CA sensor collected on the side which the melting gel was applied to (a) before application and (b) after application are remarkably similar. The spectra are shown in Fig. 4(a) and (b), and the peak assignments for the spectra are listed in Table 1.

For comparison, spectra were collected from the melting gel itself. One such representative spectrum is displayed in Fig. 5. The peak assignments for this spectrum are listed in Table 2. The assignments from Table 1 for the additional peaks attributed to the melting gel applied to the PANI-CA film agree with the assignments for the peaks in the pure melting gel spectrum.

Fig. 6 displays video frames captured during an acetone headspace exposure test of a PANI-CA film that has had the 65% MTES – 35% DMDES melting gel applied to it. Fig. 6(a) is the video frame immediately following introduction of the sample to the environment in the conical flask, and Fig. 6(b) is the video frame 150 s later.

4. Discussion

After trying other compositions of MTES and DMDES, the composition selected for the further study described here was 65% MTES-35% DMDES. Some other compositions did not reach a low viscosity suitable for application with a paint brush, which made the coatings too thick. In other cases, the gels required higher temperatures for consolidation. Consolidation is a necessary step to eliminate the tackiness of the gel and create a seal as desired here. Even though the composition with 65% MTES-35% DMDES consolidates at a reasonable temperature in 24 h, there is some tackiness left. Further research is planned to eliminate this tackiness entirely and may require addition of a third component such as tetra ethoxysilane (TEOS).

Nevertheless, it appears that this composition 65% MTES-35% DMDES is a favorable combination which gives a compact network with no accessible surface area and a high concentration of methyl groups on the surface. At higher concentrations of DMDES, meaning more methyl groups, some of the methyl groups may remain in the bulk of the coating, resulting in a network, which is less cross-

Fig. 3. Sample of PANI-CA coated with melting gel after consolidation treatment.

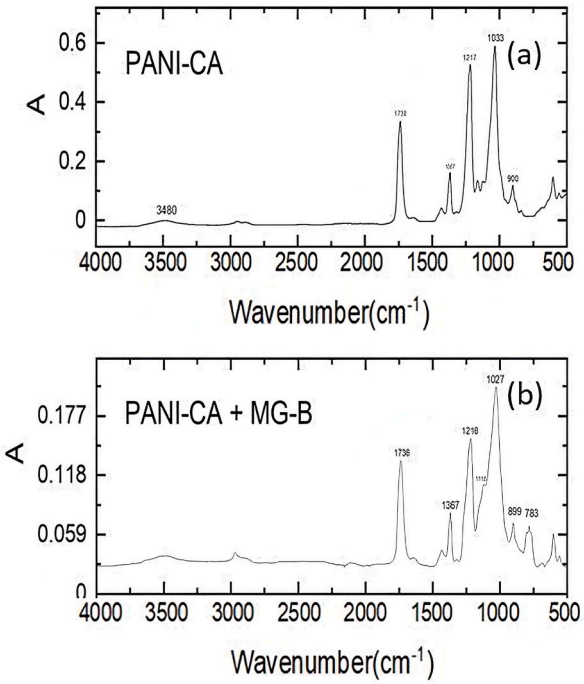

Fig. 4. FTIR spectrum of PANI-CA before (a) and after (b) melting gel application.

Table 1
Peak assignments for PANI-CA FTIR Spectrum (Saad et al., 2020).

Assignment	Wavenumber (cm^{-1}) PANI-CA	Wavenumber (cm^{-1}) PANI-CA + MG-B
νs Si–*O*–Si	–	783
ν OH	900	899
ν C–OH, ν_{as} C–O–C	**1033**	**1027**
ν_{as} Si–O–Si	**-**	**1118**
ν C–O	**1217**	**1216**
δ C–H	**1367**	**1367**
ν C=O	**1738**	**1736**
ν OH	**3480**	**-**

The differences between FTIR spectra of the PANI-CA films before and after the application of the melting gel are minor, including a difference of only a few wavenumbers for –OH and C–OH vibrations. In the spectrum for the PANI-CA with the melting gel, there are additional peaks at 783 and 1118 cm^{-1} due to the silica network, the symmetric Si–*O*–Si and asymmetric Si–*O*–Si vibrations.

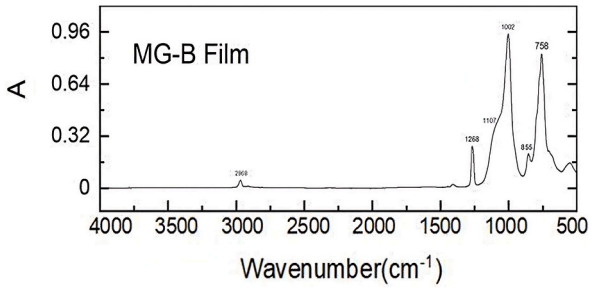

Fig. 5. FTIR spectrum of 65% MTES-35% DMDES melting gel alone.

linked. After consolidation, the compositions with more DMDES have some porosity accessible to nitrogen, which leads to a low but measurable BET surface area and a slightly lower contact angle.

The key requirement for protecting the PANI-CA sensor with melting gel is that the melting gel cannot interfere with the

Table 2
Peak assignments for melting gel FTIR Spectrum (Saad et al., 2020).

Assignment	Wavenumber (cm^{-1}) Melting gel
ν*s* Si–*O*–Si	**758**
r Si–O	**855**
ν_{as} Si–*O*–Si	**1002**
ν_{as} Si–*O*–Si	**1107**
δ CH_3	**1268**
ν_{as} CH_3	**2968**

As is typical for the FTIR spectra for melting gels, there are peaks associated with the silica network (758, 855, 1002, and 1107 cm^{-1}). Important peak assignments related to the composition of this gel are the peaks associated with the methyl group. The selection of the melting gel composition 65% MTES – 35% DMDES was based on the presence of the methyl groups that produce the hydrophobic surface that can protect the underlying PANI-CA sensor.

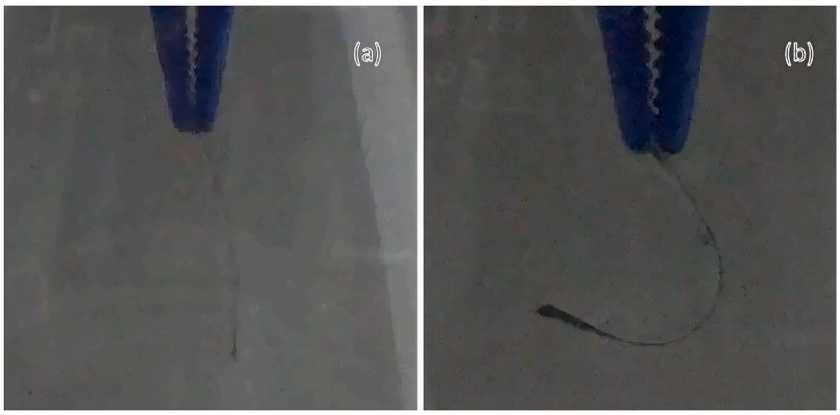

Fig. 6. Images of the PANI-CA-melting gel composite immediately upon exposure to gaseous acetone (a) and after 150 s of exposure.

functioning of the sensor. While the melting gel must form a hermetic seal to fulfill its primary function, it still must be flexible to allow the sensor to respond to biomarkers in low concentrations. Preliminary observations of the sensing functionality of the full PANI-CA-melting gel composite are encouraging and are being followed up with quantitative measurements.

5. Conclusions

This study has shown that a melting gel, which is an organic-inorganic hybrid silicate, can be applied to a PANI-CA sensor without obvious detrimental effects. The melting gel adheres to the PANI-CA film, giving a uniform, transparent coating. The adhesion is sufficient to allow PANI-CA film to bend without cracking the melting gel coating as determined by visual inspection of samples with between 0.06 mm and 0.12 mm thick melting gel coatings. These melting gel coatings were applied with a paint brush to one side of the PANI-CA strips, which were 40 mm by 3 mm rectangles. FTIR spectra indicate almost no chemical effect of the melting gel on the PANI-CA film, leading to the conclusion that the sensor's molecular structure and, consequently, its sensitivity is not impacted by the melting gel coating. This is supported by preliminary tests of the PANI-CA-melting gel composite in the headspace above acetone in a conical flask. In terms of a working device, the gel coating serves its role as a hermetic barrier without interfering with the ability of PANI-CA to respond to gaseous biomarkers.

Declaration of competing interest

The authors declare that they have no known competing financial interests or personal relationships that could have appeared to influence the work reported in this paper.

Data availability

Data will be made available on request.

Acknowledgments

This study was supported by the National Science Foundation SCH-INT grant number IIS 2014506. https://www.nsf.gov. The funders had no role in study design, data collection and analysis, decision to publish, or preparation of the manuscript.

References

Alessi, S. M., Barnett, N. P., & Petry, N. M. (2017). Experiences with SCRAMx alcohol monitoring technology in 100 alcohol treatment outpatients. *Drug and Alcohol Dependence, 178*, 417–424. https://doi.org/10.1016/j.drugalcdep.2017.05.031

Annerino, A., Faltas, M., Srinivasan, M., & Gouma, P.-I. (2022). Towards skin-acetone monitors with selective sensitivity: Dynamics of PANI-CA films. *PLoS One, 17*(4), Article e0267311. https://doi.org/10.1371/journal.pone.0267311

Aparicio, M., Jitianu, A., Rodriguez, G., Al-Marzoki, K., Jitianu, M., Mosa, J., & Klein, L. C. (2017). Thickness-properties synergy in organic–inorganic consolidated melting-gel coatings for protection of 304 stainless steel in NaCl solutions. *Surface and Coatings Technology, 315*, 426–435. https://doi.org/10.1016/j.surfcoat.2017.02.059

Bag, A., & Lee, N.-E. (2021). Recent advancements in development of wearable gas sensors. *Advanced Materials Technologies, 6*(3), Article 2000883. https://doi.org/10.1002/admt.202000883

Biscay, J., Findlay, E., & Dennany, L. (2021). Electrochemical monitoring of alcohol in sweat. *Talanta, 224*, Article 121815. https://doi.org/10.1016/j.talanta.2020.121815

Candell, L., Shaw, G., & Thompson, K. (2020). Model and personal sensor for metabolic tracking and optimization. *Lincoln Laboratory Journal, 24*(1), 114–140.

Gambino, L., Jitianu, A., & Klein, L. C. (2012). Dielectric behavior of organically modified siloxane melting gels. *Journal of Non-crystalline Solids, 358*(24), 3501–3504. https://doi.org/10.1016/j.jnoncrysol.2012.01.002

Ganguly, A., Rice, P., Lin, K.-C., Muthukumar, S., & Prasad, S. (2020). A combinatorial electrochemical biosensor for sweat biomarker benchmarking. *Slas technology: Translating Life Sciences Innovation, 25*(1), 25–32. https://doi.org/10.1177/2472630319882003

Gouma, P., & Stanacevic, M. (2011). Selective nanosensor array microsystem for exhaled breath analysis. *Procedia Engineering, 25*, 1557–1560. https://doi.org/10.1016/j.proeng.2011.12.385

He, X., Liu, Q., Wang, J., & Chen, H. (2019). Wearable gas/strain sensors based on reduced graphene oxide/linen fabrics. *Frontiers of Materials Science, 13*(3), 305–313. https://doi.org/10.1007/s11706-019-0472-1

Jitianu, A., Doyle, J., Amatucci, G., & Klein, L. C. (2010). Methyl modified siloxane melting gels for hydrophobic films. *Journal of Sol-Gel Science and Technology, 53*(2), 272–279. https://doi.org/10.1007/s10971-009-2087-y

Jitianu, A., Lammers, K., Arbuckle-Kiel, G. A., & Klein, L. C. (2012). Thermal analysis of organically modified siloxane melting gels. *Journal of Thermal Analysis and Calorimetry, 107*(3), 1039–1045. https://doi.org/10.1007/s10973-011-2024-5

Kang, N., Lin, F., Zhao, W., Lombardi, J. P., Almihdhar, M., Liu, K., Yan, S., Kim, J., Luo, J., Hsiao, B. S., Poliks, M., & Zhong, C.-J. (2016). Nanoparticle–nanofibrous membranes as scaffolds for flexible sweat sensors. *ACS Sensors, 1*(8), 1060–1069. https://doi.org/10.1021/acssensors.6b00414

Klein, L. C., & Jitianu, A. (2010). Organic–inorganic hybrid melting gels. *Journal of Sol-Gel Science and Technology, 55*(1), 86–93. https://doi.org/10.1007/s10971-010-2219-4

Klein, L. C., & Jitianu, A. (2014). Encapsulating battery components with melting gels. In *Advances in materials science for environmental and energy technologies III* (pp. 279–286). John Wiley & Sons, Ltd. https://doi.org/10.1002/9781118996652.ch23.

Klous, L., De Ruiter, C., Alkemade, P., Daanen, H., & Gerrett, N. (2020). Sweat rate and sweat composition during heat acclimation. *Journal of Thermal Biology, 93*, Article 102697. https://doi.org/10.1016/j.jtherbio.2020.102697

Manolis, A. (1983). The diagnostic potential of breath analysis. *Clinical Chemistry, 29*(1), 5–15. https://doi.org/10.1093/clinchem/29.1.5

Miekisch, W., Schubert, J. K., & Noeldge-Schomburg, G. F. E. (2004). Diagnostic potential of breath analysis—focus on volatile organic compounds. *Clinica Chimica Acta, 347*(1), 25–39. https://doi.org/10.1016/j.cccn.2004.04.023

Mojtabavi, M., Jodhani, G., Rao, R., Zhang, J., & Gouma, P. (2016). A PANI–Cellulose acetate composite as a selective and sensitive chemomechanical actuator for acetone detection. *Advanced Device Materials, 2*(1), 1–7. https://doi.org/10.1080/20550308.2016.1198559

Morgan, R. M., Patterson, M. J., & Nimmo, M. A. (2004). Acute effects of dehydration on sweat composition in men during prolonged exercise in the heat. *Acta Physiologica Scandinavica, 182*(1), 37–43. https://doi.org/10.1111/j.1365-201X.2004.01305.x

Mörk, A.-K., & Johanson, G. (2006). A human physiological model describing acetone kinetics in blood and breath during various levels of physical exercise. *Toxicology Letters, 164*(1), 6–15. https://doi.org/10.1016/j.toxlet.2005.11.005

Patterson, M. J., Galloway, S. D. R., & Nimmo, M. A. (2002). Effect of induced metabolic alkalosis on sweat composition in men. *Acta Physiologica Scandinavica, 174*(1), 41–46. https://doi.org/10.1046/j.1365-201x.2002.00927.x

Raghu, A. V., Karuppanan, K. K., Nampoothiri, J., & Pullithadathil, B. (2019). Wearable, flexible ethanol gas sensor based on TiO2 nanoparticles-grafted 2D-titanium carbide nanosheets. *ACS Applied Nano Materials, 2*(3), 1152–1163. https://doi.org/10.1021/acsanm.8b01975

Saad, N., Chaaban, M., Patra, D., Ghanem, A., & El-Rassy, H. (2020). Molecularly imprinted phenyl-functionalized silica aerogels: Selective adsorbents for methylxanthines and PAHs. *Microporous and Mesoporous Materials, 292*, Article 109759. https://doi.org/10.1016/j.micromeso.2019.109759

Singh, E., Meyyappan, M., & Nalwa, H. S. (2017). Flexible graphene-based wearable gas and chemical sensors. *ACS Applied Materials & Interfaces, 9*(40), 34544–34586. https://doi.org/10.1021/acsami.7b07063

Solga, S. F., Alkhuraishe, A., Cope, K., Tabesh, A., Clark, J. M., Torbenson, M., Schwartz, P., Magnuson, T., Diehl, A. M., & Risby, T. H. (2006). Breath biomarkers and non-alcoholic fatty liver disease: Preliminary observations. *Biomarkers, 11*(2), 174–183. https://doi.org/10.1080/13547500500421070

Thirumalaikumar, S., Douthwaite, M., & Georgiou, P. (2021). Design of a calorimetric flow rate sensor for on-body sweat monitoring. *2021 IEEE International Symposium on Circuits and Systems (ISCAS)*, 1–5. https://doi.org/10.1109/ISCAS51556.2021.9401411

Toyooka, T., Hiyama, S., & Yamada, Y. (2013). A prototype portable breath acetone analyzer for monitoring fat loss. *Journal of Breath Research, 7*(3), Article 036005. https://doi.org/10.1088/1752-7155/7/3/036005

Turner, C., Parekh, B., Walton, C., Španěl, P., Smith, D., & Evans, M. (2008). An exploratory comparative study of volatile compounds in exhaled breath and emitted by skin using selected ion flow tube mass spectrometry. *Rapid Communications in Mass Spectrometry, 22*(4), 526–532. https://doi.org/10.1002/rcm.3402

Vasilescu, A., Hrinczenko, B., Swain, G. M., & Peteu, S. F. (2021). Exhaled breath biomarker sensing. *Biosensors and Bioelectronics, 182*, Article 113193. https://doi.org/10.1016/j.bios.2021.113193

Ye, M., Chien, P.-J., Toma, K., Arakawa, T., & Mitsubayashi, K. (2015). An acetone bio-sniffer (gas phase biosensor) enabling assessment of lipid metabolism from exhaled breath. *Biosensors and Bioelectronics, 73*, 208–213. https://doi.org/10.1016/j.bios.2015.04.023